Electron-Shading Characterization in a HDP Contact Etching Process Using a Patterned CHARM Wafer

J-P Carrère[1], T. Poiroux[2,3], W. Lukaszek[4], C. Vérove[1], M. Haond[1], G. Reimbold[2], G. Turban[5]

[1] Centre Commun CNET STMicroelectronics, *850, rue Jean Monnet, 38926 Crolles Cedex, France*
[2] LETI (CEA Grenoble), *17 rue des Martyrs, 38054 Grenoble Cedex 09, France.*
[3] MHS, *La Chantrerie, route de Gachet, BP 70602, 44306 Nantes Cedex 3, France.*
[4] Wafer Charging Monitors, Inc.*, 127 Marine Road, Woodside, California, USA 94062*
[5] Institut des Matériaux de Nantes, *2 rue de la Houssinière, BP 32229, 44322 Nantes Cedex 3, France.*

In this work, a CHARM-2 wafer with high aspect ratio resist patterns has been used to quantitatively characterize the electron-shading effect in a HDP oxide etch reactor. Moreover, we show by the decrease of the maximum collected current that an ion shading phenomenon also occurs for the highest aspect ratio. Finally, a careful analysis of antenna ratio effects may indicate the importance of UV assisted leakage current.

I. Introduction

To understand the origin of plasma-induced damage, useful plasma parameters such as floating potentials and J-V characteristics can be measured using the non-invasive CHARM method [1]. Moreover, in processes such as contacts or vias etching, the main charging effect is called electron-shading and is due to the presence of high aspect ratio patterns on the wafer. This phenomenon induces a positive voltage at the via bottom, because of the difference between ions and electrons velocity isotropy [2,3].

To study this effect, we have designed different resist patterns on a 200 mm CHARM™-2 wafer with an e-beam lithography. This allows to obtain realistic variable aspect ratio as high as 4, contrary to previous studies [3,4]. Considering first the potential results and next the J-V curves, we put into evidence and characterize the electron-shading effect during the oxide etching process. Finally, we analyze the antenna ratio effect, and discuss the influence of UV assisted leakage currents.

II. Experimental

CHARM™-2 is a well-known technique based on the deprogramming property of a pre-programmed EEPROM connected to a Charge Collection Electrode (CCE or antenna) [1]. In this study, we use both the results obtained on potential (Fig. 1-a) and current sensors (Fig. 1-b).
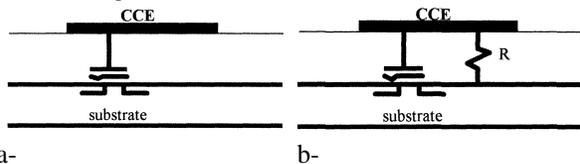

a-   b-

Figure 1. *CHARM™-2 potential sensor(a) and charge-flux sensor(b) [1].*

The potential sensors record the maximum potential difference between the antenna and the substrate and the current sensors allow the reconstruction of the J-V characteristic seen by the CCE. Negative and positive voltages and currents are recorded by distinct sensors with a different programming voltage polarity.

We have covered the whole wafer with a 0.6 µm thick resist layer and we have opened contact holes on the CCE with an e-beam lithography (LEICA VB6HR). The different resist patterns are defined to study both the contact size and the contact number effects on antenna potential and collected current.

For two given open areas on the CCE (80 and 800 µm²), we have designed contact arrays with hole sizes of 0.15, 0.30, 0.40 and 0.60 µm. For 0.40 µm contacts, we have designed arrays corresponding to open areas of 16, 80, 160, 800 and 1600 µm². Contact numbers of the different arrays are given in Table 1.

Aspect ratio	4	2	1.5	1
Size / Area	0.15 mm	0.30 mm	0.40 mm	0.60 mm
16 mm²	/	/	98	/
80 mm²	3430	882	490	196
160 mm²	/	/	980	/
800 mm²	34300	8820	4900	1960
1600 mm²	/	/	9800	/

Table 1. *Contacts number for different sizes and open areas*
.

During contact etching, a two-dimensional electron shading effect is involved, leading to large positive potentials at the contact bottom. To compare this 2D shading with a 1D effect, we have designed a structure with 25 lines of 107x0.3 µm², corresponding to an open area on the CCE of 800 µm².

All the 12 designed structures are arranged in a 4x3 dies array repeated 20 times on the wafer.

On four dies, the resist is cleared from the antennas to see the e-beam exposure effect.

The CHARM-2 wafer with the resist pattern has next been exposed to a high density plasma in a ICP oxide etch reactor. Bias and source frequencies are respectively 1.8 MHz and 2 MHz. The duration of the contact etch process has been shortened to around 10s, in order not to damage the CHARM-2 wafer.

A bare CHARM-2 wafer exposed to the same process has been used as a reference, in order to characterize the HDP plasma without resist pattern effect.

III. Results

A. Identification of the charging mechanisms

We have first compared the mean recorded positive voltages on the two CHARM-2 wafers (Fig. 2):
- **Bare wafer**: we observe a uniform potential distribution on the wafer, with a small mean voltage value (about 2V).
- **Resist patterned wafer**: the mean positive voltage has increased to a value as high as 12V.

Note that the negative voltage sensors did not respond on both wafers. The increase of the CCE potential caused by the contact pattern shows that **the electron shading effect plays a very important role for the charging potential build during contact etch.**
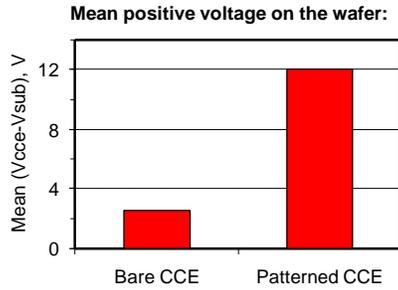
Figure 2. *Mean positive voltage recorded on a bare wafer (left) and on CCE with 0.4 μm contacts arrays (right) (corresponding open area: 1600 μm².).*
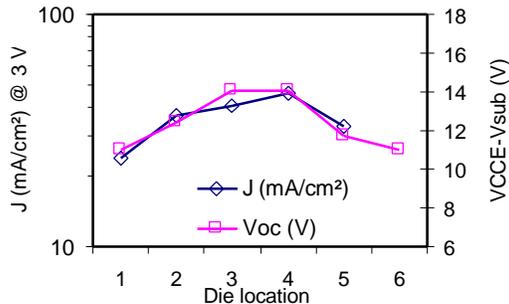
Figure 3. *Evolution of the positive voltage and maximum collected current along a patterned wafer diameter. CCE with a 0.4 μm contacts array corresponding to an open area of 1600 μm².*

Moreover, we observe on Fig. 3 a center-to-edge distribution of the radial profile of both the floating potential and the maximum collected current. This

indicates that the plasma density is not very uniform, higher at the center of the wafer than on the edge[5].

However, the center-to-edge CCE potential difference (about 2-3V) represents only 20 % of the total CCE voltage. Thus, plasma non-uniformity can not be considered as the main charging mechanism in this experiment.

B. 2D electron-shading effect characterization

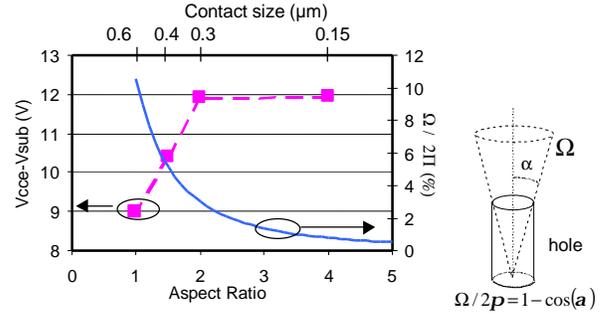By varying the contact size, we have studied the influence of the aspect ratio on the CCE potential.

Figure 4. *Evolution of the mean positive voltage versus the aspect ratio, for an open area of 800 μm².The normalized solid angle evolution is also drawn.*

Fig. 4 clearly shows that the CCE potential increases when the aspect ratio of the contact increases from 1 to 2. This behavior corresponds to a classic electron-shading phenomenon: the higher the aspect ratio, the smaller the solid angle of the pattern (Fig. 4) and so the smaller the electron flux collected at the hole bottom. This initial deficit of electrons is the cause of the increase of the CCE potential at the equilibrium. This behavior can be described by the expression [6]:

$$V_{oc}(CCE) = \frac{k.T_e}{e} . \ln\left(\frac{k_i}{k_e}\right) \qquad \text{(Equation 1)}$$

with $V_{oc}(CCE)$ the open circuit CCE voltage, T_e the electron temperature, k_e and k_i the respective electrons and ions flux shadowing factors at the hole bottom. According to this simple model, the observed CCE potentials mean that before the steady state, less than 10% of the electron flux impinges at the hole bottom for aspect ratios higher than 1. This value is consistent with the order of magnitude of the normalized solid angle of the patterns (less than 10%, Fig. 4).

We also note in Fig. 4 that the floating potential seems to saturate when the aspect ratio increases above 2. This behavior can be better understood studying the plasma J-V curves.

C. 2D electron-shading influence on J-V plots

Fig. 5 shows the different J-V plots obtained at different locations on the wafer for the same CCE configuration. Because of the J-V dispersion on the

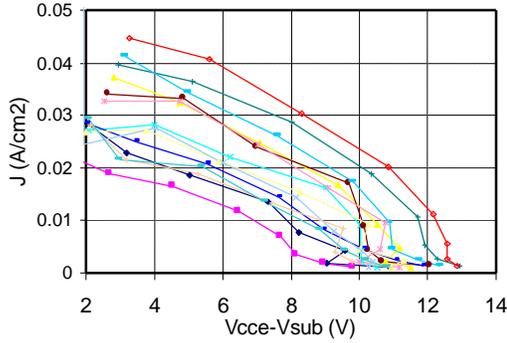wafer, we have represented the mean of the J-V plots as a function of the contacts width in Fig. 6.

Figure 5. *J-V plots for a CCE with a 0.4 μm contacts array with an equivalent open area of 1600 μm². The J-V dispersion is correlated to the plasma non-uniformity on the wafer.*
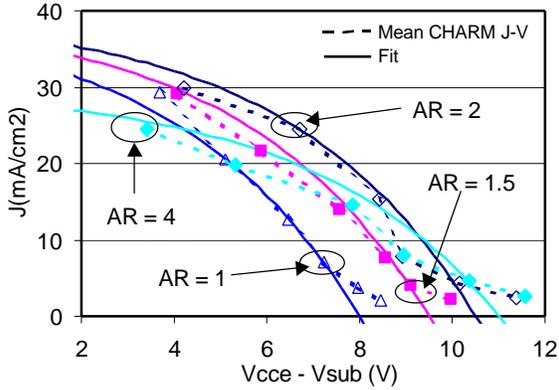

Figure 6. *Mean J-V plots versus the contacts width. The equivalent open area is 800 μm².*

We note that the behavior of the J-V can be fitted with a good approximation by the equation [7]:

$$J = k_i.J_{is}.\left(1 - \exp\left(\frac{e.(V - V_{oc})}{k.T_e}\right)\right) \quad (\textbf{Equation 2})$$

where J_{is} is the ionic current at saturation, T_e the electron temperature, V_{oc} the voltage between the CCE and the substrate in open circuit case (no current). This voltage depends on the aspect ratio as discussed in the previous paragraph. We have also introduced the parameter k_i from Eq.1 to take into account the decrease of the mean ionic saturation current for the aspect ratio of 4. Indeed, this can be explained by a shading of the ion flux (about 25%, $k_i = 0.75$) caused by the important aspect ratio. This ion flux decrease also explains why the CCE potential saturates when the aspect ratio increases from 2 to 4 (Fig. 4).

The fits of the different J-V curves have been obtained with $T_e = 4$ eV and $J_{is} = 40$ mA/cm².

Note that for the highest voltages, the experimental J-V curves diverge from the fits. This could be explained by a variation of the shadowing factors of Eq.1 with the CCE potential, and may show the limits of this simple electron-shading model.

D. 1D versus 2D electron-shading:

Fig. 7 compares the mean CCE potential measured for holes (2D) and lines (1D). We note that, for an equivalent surface of 800μm², the floating potential is higher with 0.3 µm contacts patterns than with 0.3 µm lines patterns on the CCE. This shows that the electron shading is stronger with a 2D pattern (hole) than a one-dimension one (line) for equivalent aspect ratio.

This can be also correlated to the solid angle of the pattern, smaller for a hole than a line [8]: as a consequence, the electron collection is less at the hole bottom, inducing a greater positive potential.
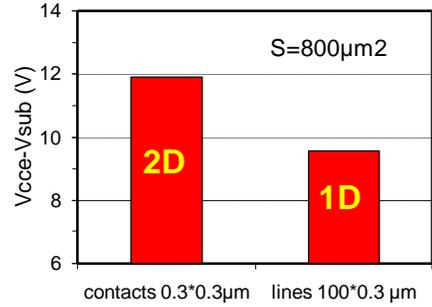

Figure 7. *Mean CCE potential versus the pattern shape (hole versus line), for an equivalent surface of 800 μm².*

E. Antenna ratio effects:

In order to study antenna ratio effect, we have varied the number of contacts on the CCE. As expected, we obtain a linear increase of the maximum collected current (I for V=3V) versus the equivalent open area (Fig. 8).

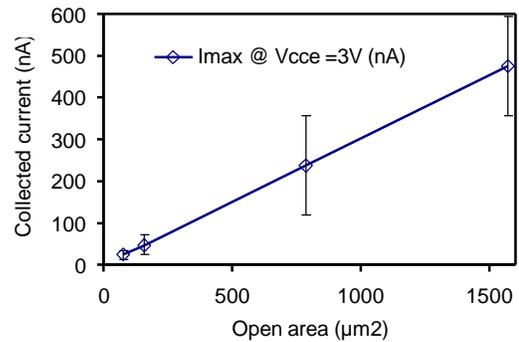**Figure 8.** *Maximum collected current versus the open area (Contact diameter: 0.4 μm).*

However, we observe a logarithmic variation of the mean CCE open circuit voltage with the open CCE area, as shown in Fig. 9. The consequence on the J-V curves is shown on Fig. 10. This behavior is unexpected*: the potential of a floating surface exposed to a plasma should be independent on the area. It should be only dependent on plasma parameters, and on the aspect ratio (electron-shading) [6].*
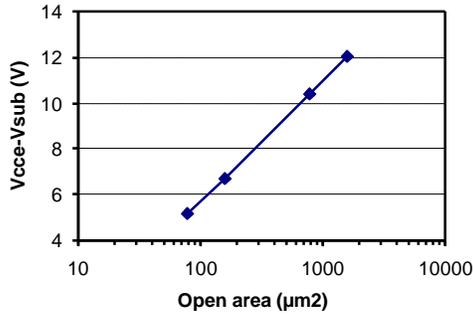
Figure 9. *Mean CCE open circuit voltage versus the open area.(Contact diameter: 0.4 μm).*
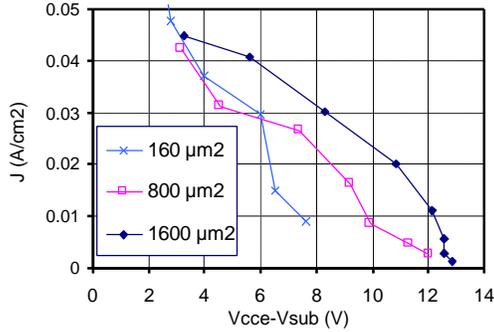

Figure 10. *J-V curves on CCE with a 0.4μm contact array, for different open areas.*

To explain this unexpected evolution of the CCE to substrate voltage with the open area, we have investigated several hypotheses.

First, this evolution cannot be explained by the difference in the e-beam exposure duration because, in that case, the response of the EEPROM with the completely cleared antennas should saturate, whereas these sensors were only exposed to a CCE voltage of around 6V.

Second, we evaluate the time needed to reach the electrical steady state between the plasma and the device. The capacitance formed by the EEPROM and the CCE with the substrate is about 5 pF. Thus, considering the measured J_{is} of 40 mA/cm², the time needed to reach a few volts with the smallest open area (16 μm²) is about 10 ms. As a consequence, the results could be explained by a transient effect of a few milliseconds, but, in that case, the positive J-V would show a severe downturn at low voltages, because the EEPROM data was converted using a charging time of 10s (process time). Since this was not observed, the recorded values are attributed to steady-state charging.

Finally, we consider a parasitic leakage between the CCE and the substrate, maybe coming from UV assisted photo-current [9]. We have computed that a parasitic resistance of around 200 MΩ would be realistic considering the range of variation of the CCE voltage with the open area. If we now correct the J-V curves of Fig. 10 considering this parasitic resistance in parallel with the current sensor resistance (Fig. 1-b), we

note on Fig. 11 that, now, the J-V curves look better superimposed whatever the open area. This leakage phenomenon could be the cause of an underestimating of the open circuit voltage observed on small open area. However, we assume that it does not significantly change the others parameters of the J-V fits, and that the J-V evolution vs. the aspect ratio is correct since the open area has been kept constant, and large (800um²).
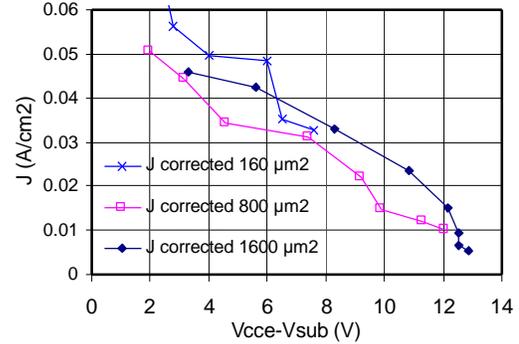

Figure 11: *J-V curves with a 0.4μm contact array for different open areas , considering a parasitic resistance of 200MΩ.*

IV. Conclusion

In this study, we have shown that electron shading can be comprehensively studied with resist patterned CHARM-2 wafers. The results we obtain on a patterned wafer in a oxide etch reactor indicate a clear shift of the J(V) curve that depends on the hole aspect ratio: the increase of the antenna potential with the aspect ratio is strong, and this shows that the electron-shading is the main charging mechanism in a contact etching process. We also observe a surprisingly strong dependence of the supposed open circuit voltage with the antenna ratio, maybe due to an UV assisted leakage. If confirmed, this point is very important since that behavior should exist in other cases of charging studies.

V. Acknowledgement

VI. References

[1]   W. Lukaszek – *"The Fundamentals of CHARM™-2"* – Technical Note 1 – Wafer Charging Monitor , Inc. – 1995.
[2]   K.P. Giapis, G.S. Hwang,- *"Pattern-Dependent Charging ..."*, Jpn. J. Appl. Phys. Vol. 37 (1998) pp.2281-2290
[3]   W. Lukaszek, J. Shields, A. Birell, *"Quantifying Via Charging Currents"*, Proc. of P2ID'97, p 123.
[4]   R Patrick et al. *"Study of Pattern Dependent Charging..."*, Proc. Of Symp. P2ID'97, p 59.
[5]   K.P. Cheung et al., J. Appl. Phys., **75** (9), 4415 (1994)
[6]   V. Vahedi, N. Benjamin, A. Perry, *"Topographical Dependence of Plasma Charging..."*, Proc of P2ID'97 , p. 41
[7]   S. Ma, JP McVittie *"Prediction of Plasma Charging..."*, Proc. Of Symp. P2ID'96, p 20.
[8]   T. Poiroux et al., Proc. of P2ID'99, pp 177-180.
[9]   C. Cismaru, J.L. Shoet, J.P. McVittie, *"Plasma Vacuum Ultraviolet Emission ..."*, Proc of P2ID'99, pp. 192-195.